

Nonequilibrium stabilization of charge states in double quantum dots

Udo Hartmann* and Frank K. Wilhelm

Physics Department and CeNS, Ludwig-Maximilians-Universität, Theresienstr. 37, D-80333 München, Germany

(Received 5 March 2004; published 28 April 2004)

We analyze the decoherence of charge states in double quantum dots due to cotunneling. The system is treated using the Bloch-Redfield generalized master equation for the Schrieffer-Wolff transformed Hamiltonian. We show that the decoherence, characterized through a relaxation τ_r and a dephasing time τ_ϕ , can be controlled through the external voltage and that the optimum point, where these times are maximum, is not necessarily in equilibrium. We outline the mechanism of this nonequilibrium-induced enhancement of lifetime and coherence. We discuss the relevance of our results for recent charge qubit experiments.

DOI: 10.1103/PhysRevB.69.161309

PACS number(s): 73.21.La, 72.70.+m, 03.67.Lx, 05.40.-a

The loss of quantum coherence is a central paradigm of modern physics. It not only governs the transition between the quantum-mechanical and the classical world, but has recently also gained practical importance in the context of engineering quantum computing devices. Decoherence naturally occurs in small quantum systems coupled to macroscopic heat baths. A huge class of such baths generates Gaussian noise and can hence be mapped on an ensemble of harmonic oscillators as in the spin-boson model.¹ This can even apply, if the fundamental degrees of freedom of the bath are fermions, as it is, e.g., the case if the bath is a linear electrical circuit,^{2,3} which is producing Gaussian Johnson-Nyquist noise.

In this Rapid Communication, we study a generically different system: a double quantum dot coupled to electronic leads. Such systems are studied as realizations of quantum bits.⁴⁻⁶ The position (either left or right dot) of an additional spin-polarized electron is used as the computational basis of a *charge* qubit as realized in Ref. 6. For another proposal of a charge qubit in semiconductors, see Ref. 7.

Our system simultaneously couples to two distinct reservoirs of real fermions. Other than oscillator bath models, this allows for the application of a voltage between these reservoirs as a new parameter for controlling decoherence. The voltage creates nonequilibrium between the baths, which to the best of our knowledge has not been studied yet in the literature on open quantum systems.

We study the dynamics of the reduced density matrix and identify the usual two modes of decoherence, dephasing and relaxation: Dephasing is the loss of phase information, manifest as the decay of coherent oscillations. This corresponds to the time evolution of the off-diagonal elements of the reduced density matrix in the energy basis. Relaxation is the process during which a quantum system exchanges energy with the environment and ends up in a stationary state. This is described through the evolution of the diagonal density matrix elements. We are going to show that, surprisingly, the charge states can be stabilized by external nonequilibrium, i.e., the relaxation time is longest at a well-defined finite voltage. We will show, that this working point is also very favorable in terms of dephasing but competes with another local maximum at zero voltage. Our theory should also have applications in other systems.

We consider a double quantum dot system with an appreciable tunnel coupling between the dots allowing for coherent molecular states in these systems.⁸ The computational basis is formed by the position states of an additional spin-polarized electron.^{6,7} A superposition can be created by variation of the interdot coupling. In order to stabilize the charge, the coupling of the dots to the two leads is driven to weak values and the dot is tuned to the Coulomb blockade regime⁹ where sequential tunneling is suppressed through the addition energy. Even then, the system couples to the environment through cotunneling,¹⁰ the correlated exchange of two electrons with the external leads which ends up in a state with the same total charge as the initial one.

The relevant Hilbert space is spanned by four states written $|i,j\rangle$ denoting i,j additional electrons on the left and right dot, respectively. $|1,0\rangle$ and $|0,1\rangle$ define the computational basis as they are energetically accessible, the closest virtual intermediate states for cotunneling are $|v_0\rangle = |0,0\rangle$ and $|v_2\rangle = |1,1\rangle$. This model applies if all relevant energy scales of the system (ε_{as} and γ , see below) are much smaller than the charging energies to the next virtual levels (ε_{v_2} and ε_{v_0} , also below), which in turn have to be smaller than the orbital excitation of the individual dots. This can be realized in small dots.

The total Hamiltonian of this system can be written as $H = H_0 + H_1$ where $H_0 = H_{\text{sys}} + H_{\text{res}}$ describes the energy spectrum of the isolated double-dot through $H_{\text{sys}} = \varepsilon_{\text{as}}(a^{L\dagger}a^L - a^{R\dagger}a^R) - \varepsilon_{v_0}\hat{n}_{v_0} + \varepsilon_{v_2}\hat{n}_{v_2} + \gamma(a^{L\dagger}a^R + a^{R\dagger}a^L)$ and the two electronic leads $H_{\text{res}} = \sum_{\vec{k}} \varepsilon_{\vec{k}}^L b_{\vec{k}}^{L\dagger} b_{\vec{k}}^L + \sum_{\vec{k}} \varepsilon_{\vec{k}}^R b_{\vec{k}}^{R\dagger} b_{\vec{k}}^R$. The sum over the dot states only runs over the restricted Hilbert space described above, the $a^{L/R}$ act on the lowest additional electron state on either dot. The double-dot is characterized by the asymmetry energy $\varepsilon_{\text{as}} = \varepsilon_l - \varepsilon_r$ between the individual dots and the interdot tunnel coupling γ . The virtual states $|v_2\rangle$ and $|v_0\rangle$ are separated from the system by energy differences ε_{v_2} (upper virtual level) and ε_{v_0} (lower virtual level). The tunneling part $H_1 = t_c \sum_{k,n} (a_n^{L\dagger} b_k^L + a_n^L b_k^{L\dagger}) + t_c \sum_{k',m} (a_m^{R\dagger} b_{k'}^R + a_m^R b_{k'}^{R\dagger})$ describes the coupling of each dot to its lead and will be treated as a perturbation. t_c represents the tunnel matrix elements between the dots and the leads. It can be absorbed in a tun-

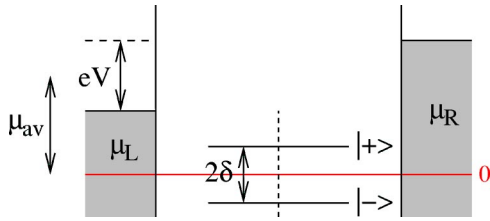


FIG. 1. (Color online) Sketch of the considered artificial molecule in the Coulomb blockade regime, where 2δ is the level splitting and $V = \mu_R - \mu_L$ the bias voltage, that is applied between the two leads (hatched). The virtual states $|v_2\rangle$ and $|v_0\rangle$ are outside the plotted energy range.

neling rate $\hbar\Gamma = 2\pi t_c^2 N(\epsilon_F)$. This has to be chosen small such that the Kondo temperature is low $T_K \ll T$ and perturbation theory holds, e.g., $\Gamma = 10^9$ Hz. Figure 1 shows a sketch of the setup.

From now on, we use the basis of molecular states obtained by diagonalizing H_{sys} with splitting $2\delta = 2\sqrt{\epsilon_{\text{as}}^2 + \gamma^2}$. In order to treat cotunneling by leading-order perturbation theory, we rewrite H_1 using a Schrieffer-Wolff transformation.¹¹ This removes the transitions to the virtual states and generates an effective Hamiltonian containing indirect transition terms between the molecular states. A more detailed description of our calculation is given in Refs. 5 and 12. The final Hamiltonian is of the form $H = H_0 + H'_1$ where

$$H'_1 = \sum_{c,d} \alpha_c^\dagger \alpha_d \left[\sum_{Y,Y',\vec{k},\vec{k}'} H_{\vec{k},\vec{k}',c,d}^{Y,Y'} b_{\vec{k}}^{Y\dagger} b_{\vec{k}'}^{Y'} + \sum_{Y,Y',\vec{k},\vec{k}'} H_{\vec{k},\vec{k}',c,d}^{Y,Y'} b_{\vec{k}}^Y b_{\vec{k}'}^{Y'\dagger} \right], \quad (1)$$

where Y and Y' denote right or left lead, the α s describe molecular states and the $H_{\vec{k},\vec{k}',c,d}^{Y,Y'}$ are given through 2nd order perturbation theory, i.e., they are of $O(\Gamma^2)$. Note, that H'_1 conserves the particle number because it acts upon the double-dot by injecting *and* extracting an electron in a single step. The terms with $Y \neq Y'$ transfer charge between different reservoirs and is potentially relevant for systems other than quantum dots as well.

We study the open system dynamics in the case of a time-independent Hamiltonian with a fully general initial reduced density matrix. We use the well-established and controlled Bloch-Redfield,¹³ which has been demonstrated to work down to low temperature for certain models.¹⁴ It involves a Born approximation in H'_1 , i.e., it captures all cotunneling processes in lowest nonvanishing order. The Redfield equations¹⁵ for the elements of the reduced density matrix ρ in the eigenstate basis of H_{sys} (i.e., the molecular basis) read

$$\dot{\rho}_{nm}(t) = -i\omega_{nm}\rho_{nm}(t) - \sum_{k,l} R_{nmkl}\rho_{kl}(t), \quad (2)$$

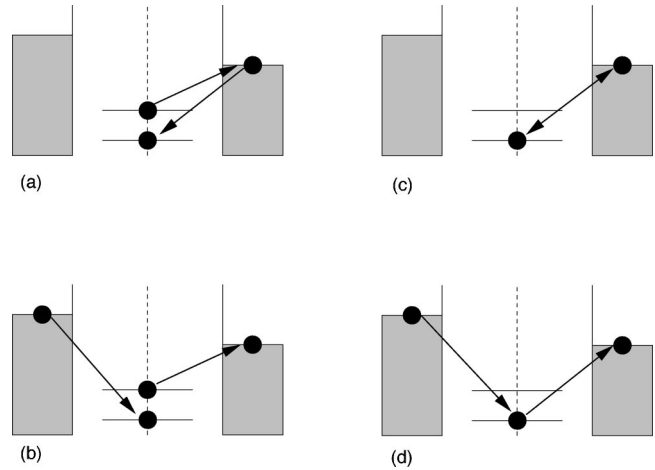


FIG. 2. Examples for relevant processes in the system: (a) a relaxation process that carries no current, (b) a relaxation process with current, (c) a pure dephasing process without current flow, and (d) a current-carrying dephasing process.

where $\omega_{nm} = (E_n - E_m)/\hbar$ and the Redfield tensor elements R_{nmkl} are composed of golden rule rates describing different cotunneling processes, which are essentially independent due to the low symmetry of the system. Each contribution has a typical cotunneling structure.^{5,12} An overview of the most important processes is given below. n, m, k and l can be either $+$ (excited molecular state) or $-$ (molecular ground state) with according energies E_{\pm} . This type of perturbative analysis is only valid above the Kondo temperature T_K ,¹⁶ which can be easily driven to low values by pinching off the tunneling barrier to the leads.

From the formal solution of Eq. (2) we can identify the relaxation and dephasing rates as

$$\Gamma_r = \text{Re}(R_{++++} + R_{----}) = \frac{1}{\tau_r}, \quad (3)$$

$$\Gamma_\phi = \text{Re}(R_{+-+-}) = \text{Re}(R_{-+ -+}) = \frac{1}{\tau_\phi}. \quad (4)$$

The transition frequencies ω_{nm} are weakly shifted.

Figure 2 shows a choice of processes entering the Redfield tensor. All processes contribute to dephasing, because the phase of an electron, which is injected from the reservoirs, is always random. Figures (a) and (b) illustrate relaxation processes. Only (b) contributes to the current, i.e., in general the *relaxation* rate must not be confused with the cotunneling *current*. In (c) and (d) two pure dephasing processes are presented; only (d) contributes to the current flow. In general, processes without current can emerge, if the cotunneling processes take place between a *single* lead and the two-state system (TSS). The *observable* current is then given by the difference of current-carrying processes in forward and backward direction. We have evaluated the rates entering Eqs. (3) and (4) using $H_{\vec{k},\vec{k}',c,d}^{Y,Y'}$. Due to the high number of terms, details are not shown and will be given elsewhere.¹²

We now turn to the discussion of our results, starting with the relaxation time τ_r . We observe in Fig. 3 that for an

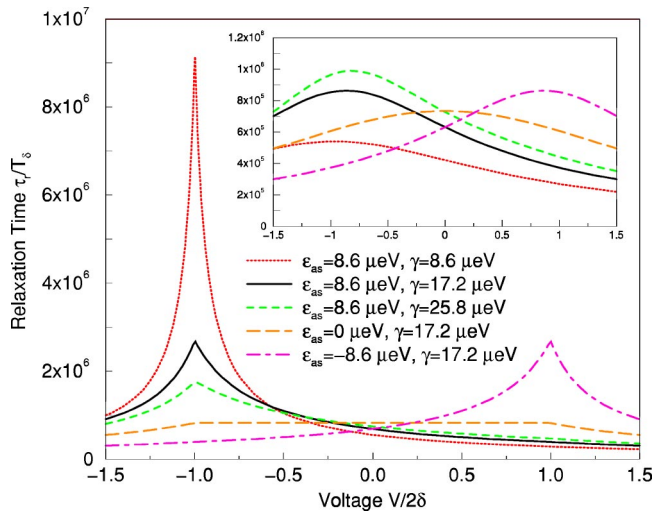


FIG. 3. (Color online) Relaxation time τ_r in units of $T_\delta = 2\pi\hbar/2\delta$, the period of coherent oscillations between the two molecular states. Different values of ϵ_{as} and γ are taken, when the bias voltage $V/2\delta$ is varied [with $\mu_{av} = (\mu_R + \mu_L)/2 = 75.832 \mu\text{eV}$ and $k_B T/\mu_{av} = 1.136 \times 10^{-3}$]; inset: $k_B T/\mu_{av} = 0.159$.

asymmetric TSS, i.e., for $\epsilon_{as} \neq 0$, there is a pronounced peak of the relaxation time at $V = -\text{sgn}(\epsilon_{as})2\delta$, where $V = \mu_R - \mu_L$, i.e., the sign has to be chosen with opposite polarity to the asymmetry energy. This means in particular that the relaxation is minimal far away from equilibrium. This is the central result of our paper. It is most clearly visible for $T \ll 2\delta$, but obviously still dominates the calculated result for temperatures $T \approx 2\delta$, as it can be seen in the insets of Figs. 3 and 4. In order to remain in the cotunneling regime, the voltages are still quite small as compared to the excitation energy to the next charge states ϵ_{v_2} and ϵ_{v_0} , but on the order of the molecular level splitting, i.e. $|V| \approx 2\delta \ll \epsilon_{v_2}, \epsilon_{v_0}$. For quantum computation, achieving a maximum relaxation time is, e.g., appreciable during *read out*.²

Although surprising, it can be understood from the analysis of the different rates, that $V=0$ does not necessarily imply the lowest relaxation rate. At $V=0$ there is no *net* current, i.e., no *net* exchange of particles in the ensemble average, however, this is achieved by the cancellation of finite currents of equal size in forward and backward direction. These currents are rather small⁵ such that current heating is reduced to a minimum. To τ_r , Eq. (3), such current-carrying processes contribute with *equal* sign—the system relaxes no matter to which reservoir. On top of this, one also has to take into account the aforementioned current-less relaxation channels.

The appearance of the peaks as preferred stable points in Fig. 3 can be understood based on the analysis of the current-carrying processes, [e.g. Figs. 2(b) and 2(d)] as schematically shown in Fig. 5. At low voltages, $|V| < 2\delta$, the system relaxes into a thermal state close to the ground state. Relaxation takes place by spontaneous emission of energy into the environment and creation of an electron-hole pair in the leads. This pair can recombine through the electrical circuit which fixes the electrochemical potentials. This leads to elec-

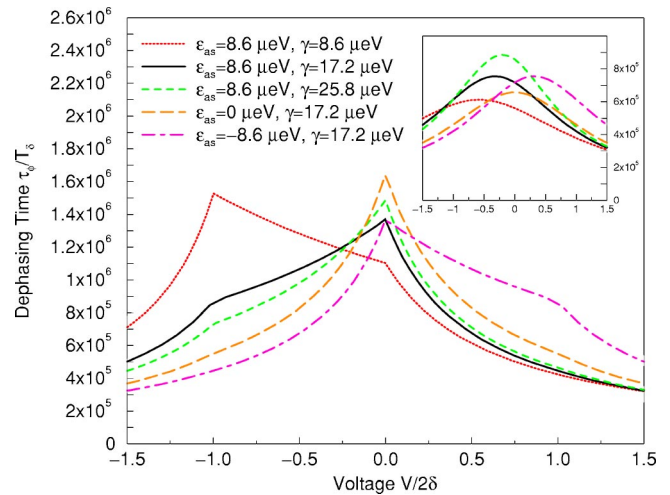


FIG. 4. (Color online) Dephasing time τ_ϕ in the same units as in the previous figure for different values of ϵ_{as} and γ , when the bias voltage $V/2\delta$ is varied [with $\mu_{av} = (\mu_R + \mu_L)/2 = 75.832 \mu\text{eV}$ and $k_B T/\mu_{av} = 1.136 \times 10^{-3}$]; inset: $k_B T/\mu_{av} = 0.159$.

trical current. As the voltage is increased away from $V=0$, emission processes which lead to a current *against* the polarity of the source are suppressed, the others are enhanced, see Figs. 5(I) and 5(II). Depending on the asymmetry of the double dot, i.e., on the weight of the excited state on the left and the right dot, this leads to an enhancement or a suppression of the rate. At $|V| \geq 2\delta$, the emission processes against the source are completely blocked: the dot relaxation does not provide enough energy to overcome the electromotive force. The rate vanishes *linearly* as a function of voltage reflecting the size of the available phase space for cotunneling, see Fig. 5.

At higher voltages, $|V| \geq 2\delta$, inelastic cotunneling¹⁷ sets in, see Figs. 5(III) and 5(IV): The source provides enough energy to even excite the double dot, creating a nonequilibrium steady-state population of the molecular levels. Hence, inelastic cotunneling provides a way for the dot to *absorb* energy from the environment even at low temperature. This process can be experimentally identified by a sharp increase of the current.^{5,17}

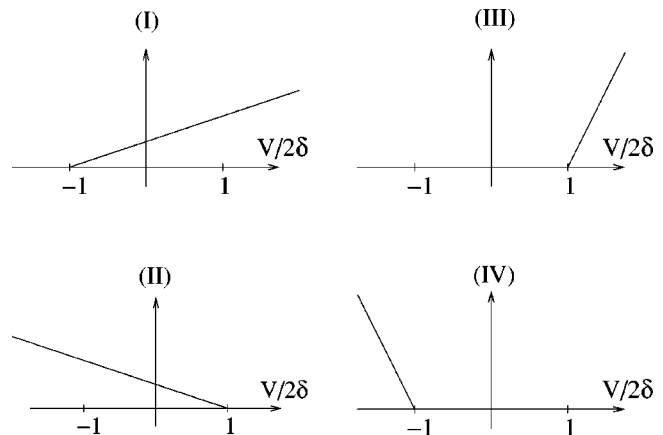


FIG. 5. Qualitative voltage dependence of the rates of emission [(I), (II)] and absorption [(III), (IV)] processes; see text; these rates do not correspond to the processes in Fig. 2.

Hence, at $V = \pm 2\delta$, three of the four processes depicted in Fig. 5 vanish at low temperatures, whereas at $V=0$ only two vanish. The linear voltage dependence of the rates leads to the rather sharp cusps seen in Fig. 3. This behavior is smeared out at higher temperatures by thermal fluctuations. The peak height is set by the remaining processes: Energy emission *with* the source and currentless relaxation, Fig. 2 (a). As explained above, the relative weight of the former strongly depends on the weight of the excited molecular state on the individual dots and thus is responsible for the strong asymmetry of the peaks in Fig. 3 for different asymmetry energies.

Finally, we analyze the properties of the dephasing time τ_ϕ as a function of the bias voltage. The total dephasing rate contains relaxing as well as flipless (“elastic”) processes. We hence observe in Fig. 4 a peak structure at $V = -\text{sgn}(\epsilon_{as})2\delta$ as in the relaxation time, Fig. 3, and a similar peak at $V=0$. The latter can be understood from the suppression of flipless processes (energy exchange 0) in an analogous way to the relaxation peak in Fig. 3 (energy exchange 2δ). At low asymmetry energy $\epsilon_{as} < \gamma$, the dephasing time at $V=0$ is longest. At high asymmetry $\epsilon_{as} > \gamma$ and at the nonequilibrium working point $V = -\text{sgn}(\epsilon_{as})2\delta$, τ_ϕ is even longer. In general, this indicates the existence of two preferable working points for quantum computation: One *in* equilibrium, the other again *far from* equilibrium. As also already seen in the inset of Fig. 3, the voltage dependence at higher temperature is here smeared out and the peaks merge.

A measurement of the relaxation and dephasing times

should be feasible either by a time-resolved measurement of $\langle \sigma_z(t) \rangle$, e.g., through a single-electron transistor or point contact,¹⁸ the saturation broadening method¹⁹ or resonance schemes such as proposed in Ref. 20 for spins.

Note that parts of the double-dot literature focus on decoherence through phonons or photons (see Refs. 8,21–23), whereas we focus on the cotunneling, which becomes relevant when phonons are suppressed by a cavity.²⁴ If the *spin* in a dot is used as qubit,^{18,25} cotunneling serves as an indirect contribution to decoherence.

To conclude, we have studied the decoherence of charge states in a double quantum dot due to cotunneling. We have shown that decoherence can be controlled through a bias voltage V (and thus creating a nonequilibrium situation) between the two fermionic baths. In particular, the optimum working point for read out and potentially also for operation of the qubit can be in an out-of-equilibrium situation at a voltage $V = -\text{sgn}(\epsilon_{as})2\delta$. We have given a consistent physical interpretation of our findings in terms of stability and phase space. This effect of stabilization through nonequilibrium should potentially be significant for other qubit candidates as well.

We thank J. von Delft, L. Borda, J. König, M.J. Storcz, A.W. Holleitner, A.K. Hüttel, and E.M. Weig for clarifying discussions. Work supported by SFB 631 of the DFG and in part by the National Security Agency (NSA) and Advanced Research and Development Activity (ARDA) under Army Research Office (ARO) contract number P-43385-PH-QC.

*E-mail address: hartmann@theorie.physik.uni-muenchen.de

¹A.J. Leggett, S. Chakravarty, A.T. Dorsey, M.P.A. Fisher, A. Garg, and W. Zwerger, *Rev. Mod. Phys.* **59**, 1 (1987).

²C.H. van der Wal, F.K. Wilhelm, C.J.P.M. Harmans, and J.E. Mooij, *Eur. Phys. J. B* **31**, 111 (2003).

³See, e.g., F.K. Wilhelm, G. Schön, and G.T. Zimanyi, *Phys. Rev. Lett.* **87**, 136802 (2001).

⁴R.H. Blick and H. Lorenz, *Proceedings of the IEEE International Symposium on Circuits and Systems*, **I245** (2000).

⁵U. Hartmann and F.K. Wilhelm, *Phys. Status Solidi B* **233**, 385 (2002); U. Hartmann and F.K. Wilhelm, *Phys. Rev. B* **67**, 161307(R) (2003).

⁶T. Hayashi, T. Fujisawa, H.D. Cheong, Y.H. Jeong, and Y. Hirayama, *Phys. Rev. Lett.* **91**, 226804 (2003).

⁷L.C.L. Hollenberg, A.S. Dzurak, C. Wellard, A.R. Hamilton, D.J. Reilly, G.J. Milburn, and R.G. Clark, *Phys. Rev. B* **69**, 113301 (2004).

⁸T.H. Oosterkamp, T. Fujisawa, W.G. van der Wiel, K. Ishibashi, R.V. Hijman, S. Tarucha, and L.P. Kouwenhoven, *Nature (London)* **395**, 873 (1998).

⁹W.G. van der Wiel, S. De Franceschi, J.M. Elzerman, T. Fujisawa, S. Tarucha, and L.P. Kouwenhoven, *Rev. Mod. Phys.* **75**, 1 (2003).

¹⁰D.V. Averin and Y.V. Nazarov, in *Single Charge Tunneling*, Vol. 294 of *NATO Advanced Study Institute, Series B: Physics*, edited by H. Grabert and M.H. Devoret (Plenum, New York, 1992), pp. 217–247.

¹¹J.R. Schrieffer and P.A. Wolff, *Phys. Rev.* **149**, 491 (1966).

¹²U. Hartmann, Master’s thesis, University of Bohn, 2002.

¹³P.N. Agyres and P.L. Kelley, *Phys. Rev.* **134**, A98 (1964).

¹⁴L. Hartmann, I. Goychuk, M. Grifoni, and P. Hänggi, *Phys. Rev. E* **61**, R4687 (2000).

¹⁵U. Weiss, *Quantum Dissipative Systems*, 2nd ed. (World Scientific, Singapore, 1999).

¹⁶F.D.M. Haldane, *Phys. Rev. Lett.* **40**, 416 (1978).

¹⁷S. De Franceschi, S. Sasaki, J.M. Elzerman, W.G. van der Wiel, S. Tarucha, and L.P. Kouwenhoven, *Phys. Rev. Lett.* **86**, 878 (2001).

¹⁸J.M. Elzerman, R. Hanson, J.S. Greidanus, L.H. Willems van Beveren, S. De Franceschi, L.M.K. Vandersypen, S. Tarucha, and L.P. Kouwenhoven, *Phys. Rev. B* **67**, 161308(R) (2003).

¹⁹M.C. Goorden and F.K. Wilhelm, *Phys. Rev. B* **68**, 012508 (2003).

²⁰H.-A. Engel and D. Loss, *Phys. Rev. Lett.* **86**, 4648 (2001); *Phys. Rev. B* **65**, 195321 (2002).

²¹H. Qin, A.W. Holleitner, K. Eberl, and R.H. Blick, *Phys. Rev. B* **64**, 241302 (2001).

²²B.L. Hazelzet, M.R. Wegewijs, T.H. Stoof, and Yu.V. Nazarov, *Phys. Rev. B* **63**, 165313 (2001).

²³T. Brandes and B. Kramer, *Phys. Rev. Lett.* **83**, 3021 (1999).

²⁴J. Kirschbaum, E.M. Höbberger, R.H. Blick, W. Wegscheider, and M. Bichler, *Appl. Phys. Lett.* **81**, 280 (2002).

²⁵D. Loss and D.P. DiVincenzo, *Phys. Rev. A* **57**, 120 (1998).